American Mineralogist, Volume 66, pages 315-323, 1981

High-pressure structural study of diopside

LOUISE LEVIEN[1] AND CHARLES T. PREWITT

Department of Earth and Space Sciences
State University of New York
Stony Brook, New York 11794

Abstract

High-pressure structural studies performed on diopside at five pressures between 1 atm and 53 kbar show that the three polyhedra that comprise the structure, M(1), M(2), and Si, decrease irregularly in size. The polyhedral volumes of M(1) and M(2) both decrease approximately 5%, whereas that of Si decreases only 1%. Comparison of high-pressure structural changes of diopside and fassaite (another clinopyroxene) shows substantial differences, with diopside showing less tetrahedral and M(1) compression and more silicate-chain kinking. Unit-cell parameters of diopside change from $a = 9.7456(7)$, $b = 8.9198(8)$, $c = 5.2516(5)$Å and $\beta = 105.86(1)°$ at 1 atm to $a = 9.612(2)$, $b = 8.765(1)$, $c = 5.1793(2)$Å and $\beta = 105.32(1)°$ at 53.0 kbar. Increased pressure has very little effect on equivalent isotropic temperature factors. Some structural features show "inverse" behavior with unit-cell volume changes caused by T or P [⟨M(1)–O⟩, ⟨M(2)–O⟩, O(3)–Si–O(3), and O(3)–O(3)–O(3)], whereas others do not (the β cell parameter and ⟨Si–O⟩). The bulk modulus and its pressure derivative, calculated from a weighted fit of the P-V data to the Birch–Murnaghan equation of state, are 1.14(4) Mbar and 4.5(1.8), respectively. The compressibility of the structure is controlled by certain M(1) and M(2) bonds. The rigid M–O bonds run parallel to the least compressible direction (ϵ_1), and the most compressible M–O bonds run ⊥ to ϵ_1 and approximately 45° between the two most compressible directions, ϵ_2 and ϵ_3.

Introduction

We have chosen to study the high-pressure crystal structure of diopside to determine the structural changes that take place with pressure, and to compare these results with those of other studies to better understand such phenomena as bond strengths, atomic vibrations, phase changes, and single-crystal elasticity. We can use the high-temperature structural refinements of Cameron *et al.* (1973) and Finger and Ohashi (1976) to test Hazen and Prewitt's (1977) predictions on inverse behavior as well as make other high-temperature and -pressure comparisons. The high-pressure structural refinements of fassaite, a clinopyroxene of similar composition (Hazen and Finger, 1977b), and orthoenstatite (Ralph and Ghose, 1980) provide us with comparisons of high-pressure structural changes among similar minerals and give us information about our current abilities to predict structural behavior at pressure. Finally, reliable single-crystal elastic moduli for a monoclinic pyroxene, again of diopside composition, have been published recently (Levien *et al.*, 1979). The newly available data on both high-pressure crystal structures and elastic moduli of the same materials let us observe which structural elements are responsible for the compressibility of a mineral, and will lead eventually to more accurate models for the elastic properties of minerals as they exist within the Earth.

Experimental techniques

The sample used was a clear crystal (50 μm × 80 μm × 130 μm) of natural diopside ($Ca_{0.99}Na_{0.02}Mg_{0.98}Fe_{0.02}Al_{0.01}Si_{1.99}O_6$) from DeKalb, New York (Harvard Museum #C2392). A Weissenberg X-ray photograph showed the diffraction pattern to consist of discrete spots rather than spots with tails that are common in pyroxene diffraction patterns. After the high-pressure intensity and cell-parameter data had been obtained, the crystal was removed from the diamond cell, and room-pressure data were collected.

[1]Present address: Exxon Production Research Company, P.O. Box 2189, Houston, Texas 77001.

0003–004X/81/0304–0315$02.00

Table 1: Intensity information for diopside at five pressures

	total #data	#after av.*	#>2σ_I **	wR	R	Ext. X 10^{-4} †
1 atm	833	795	770	0.027	0.016	0.11(2) ††
23.6 kbar	887	441	342	0.036	0.035	0.11(2)
35.2 kbar	857	426	346	0.031	0.029	0.11(2)
45.5 kbar	856	426	338	0.033	0.030	0.11(2)
53.0 kbar	854	424	347	0.039	0.037	0.11(3)

*Number of data after symmetrically equivalent reflections were averaged.
**Number of data accepted in the refinement. All were greater than 2σ_I.
†Refined secondary extinction parameters.
††Parenthesized figures represent *esd's* of least units cited.

Similar techniques to those described in Levien *et al.* (1980) were used with minor modifications reported here. The diamond cell used by Levien *et al.* was of the original design described by Merrill and Bassett (1974); the cell used in this study was modified by using flat Be discs similar to those described by Hazen and Finger (1977c), and diamonds with 1 mm faces. All reported data have been collected with Mo$K\alpha$ radiation; two refinements based on data sets collected with Ag$K\alpha$ radiation gave inferior results and have been omitted. A hemisphere of integrated intensities in reciprocal space ($2° < 2\theta < 65°$) was collected on the crystal at room pressure, whereas an entire sphere of intensities ($2° < 2\theta < 90°$), except for reflections affected by the diffraction pattern of polycrystalline Be, was collected at each high pressure. The symmetrically-equivalent reflections were averaged to yield between 424 and 441 reflections for the high-pressure runs and 795 for the room-pressure experiment. One or two reflections were rejected from each high-pressure data set because of obvious overlap with diamond reflections; all other observed reflections (greater than $2\sigma_I$) were accepted in the refinements. Five reflections were rejected from the room-pressure refinement. The addition of an extinction parameter resulted in a decrease of the R values of all five refinements at the 0.005 significance level (Hamilton, 1974). The final weighted R values range from 0.027 to 0.039 (Table 1). Observed and calculated structure factors are listed in Table 2[2]; positional parameters and equivalent isotropic and anisotropic temperature factors are given in Table 3; interatomic distances and angles for the silicate tetrahedron are reported in Table 4; interatomic distances and angles for the M(1) octahedron are listed in Table 5; interatomic distances for the M(2) polyhedron are given in Table 6; and unit-cell parameters are listed in Table 7.

[2]To receive a copy of Table 2, order document AM-81-151 from the Business Office, Mineralogical Society of America, 2000 Florida Avenue, N.W., Washington, D.C. 20009. Please remit $1.00 in advance for the microfiche.

Results

Our room-pressure structural refinement of diopside is in excellent agreement with that of Clark *et al.*

Table 3: Positional and thermal parameters of diopside at pressure

	1 atm	23.6*	35.2	45.5	53.0
M(1)**					
y	0.90814(5)†	0.9092(3)	0.9090(1)	0.9094(2)	0.9097(2)
B	0.37(1)	0.38(4)	0.32(2)	0.30(3)	0.36(3)
β_{11} ††	11.3(5)	14. (1)	9. (3)	9. (3)	11. (4)
β_{22}	11.3(5)	8. (6)	12. (2)	11. (2)	14. (3)
β_{33}	30. (2)	36. (4)	28. (3)	24. (3)	28. (4)
β_{13}	2.3(7)	1. (2)	4. (2)	3. (2)	3. (3)
M(2)**					
y	0.30144(3)	0.3026(2)	0.30333(8)	0.30378(9)	0.3040(1)
B	0.635(8)	0.58(3)	0.57(1)	0.52(2)	0.56(2)
β_{11}	22.4(3)	23.6(9)	20. (2)	20. (2)	21. (2)
β_{22}	16.4(4)	8. (3)	16. (1)	13. (1)	16. (2)
β_{33}	47. (1)	53. (2)	44. (2)	39. (2)	41. (2)
β_{13}	-1.5(4)	-1. (1)	1. (1)	-0. (1)	0. (2)
Si					
x	0.28627(3)	0.28637(8)	0.28643(9)	0.2863 (1)	0.2864(1)
y	0.09330(3)	0.0941 (2)	0.09420(8)	0.09449(9)	0.0946(1)
z	0.22936(5)	0.2285 (1)	0.2282 (1)	0.2279 (1)	0.2279(1)
B	0.349(8)	0.42(3)	0.32(2)	0.30(2)	0.33(2)
β_{11}	9.7(3)	10.4(8)	8. (2)	8. (2)	8. (2)
β_{22}	11.9(4)	16. (3)	13. (1)	11. (1)	13. (2)
β_{33}	31. (1)	38. (2)	29. (2)	26. (2)	31. (2)
β_{12}	-0.5(2)	-0.4(8)	-1.1(4)	-1.4(5)	-1.1(6)
β_{13}	4.0(4)	6. (1)	4. (1)	4. (1)	4. (2)
β_{23}	-0.7(3)	-3. (2)	-0.9(8)	-1. (1)	-3. (1)
O(1)					
x	0.11550(7)	0.1152(2)	0.1153(3)	0.1150(3)	0.1147(3)
y	0.08728(7)	0.0864(5)	0.0879(2)	0.0879(2)	0.0880(3)
z	0.1422 (1)	0.1420(4)	0.1422(3)	0.1421(3)	0.1414(4)
B	0.51(1)	0.40(6)	0.47(3)	0.42(4)	0.49(5)
β_{11}	11.4(6)	14. (2)	14. (5)	10. (5)	14. (6)
β_{22}	19.2(7)	1. (8)	16. (3)	16. (4)	18. (4)
β_{33}	47. (2)	60. (5)	41. (4)	44. (5)	46. (6)
β_{12}	0.8(5)	-0. (2)	-0.0(1)	1. (1)	1. (2)
β_{13}	4.1(9)	1. (3)	4. (3)	6. (4)	8. (4)
β_{23}	1.7(9)	2. (5)	-0.0(2)	-0. (3)	-5. (3)
O(2)					
x	0.36136(7)	0.3609(2)	0.3608(3)	0.3611(3)	0.3608(4)
y	0.25013(8)	0.2515(4)	0.2529(2)	0.2534(2)	0.2542(3)
z	0.3183 (1)	0.3192(4)	0.3196(3)	0.3204(4)	0.3212(4)
B	0.65(1)	0.70(7)	0.54(3)	0.54(4)	0.54(4)
β_{11}	22.1(7)	23. (2)	15. (4)	14. (5)	15. (6)
β_{22}	17.2(7)	27. (8)	16. (3)	19. (3)	19. (4)
β_{33}	59. (2)	46. (6)	58. (5)	57. (5)	50. (6)
β_{12}	-3.9(5)	-3. (2)	-5. (1)	-6. (2)	-3. (2)
β_{13}	8. (1)	7. (3)	6. (3)	12. (4)	4. (4)
β_{23}	-3. (1)	-3. (4)	-4. (2)	-4. (3)	-3. (3)
O(3)					
x	0.35083(7)	0.3517(2)	0.3525(3)	0.3530(3)	0.3527(3)
y	0.01759(8)	0.0185(4)	0.0202(2)	0.0207(2)	0.0213(3)
z	0.9953 (1)	0.9921(4)	0.9907(3)	0.9901(4)	0.9889(4)
B	0.56(1)	0.58(6)	0.52(3)	0.44(4)	0.51(4)
β_{11}	14.7(7)	16. (2)	16. (5)	10. (5)	16. (6)
β_{22}	21.5(8)	25. (8)	20. (3)	21. (4)	20. (4)
β_{33}	48. (2)	40. (6)	41. (4)	38. (5)	39. (6)
β_{12}	-0.3(5)	-2. (2)	0. (1)	-3. (1)	-1. (2)
β_{13}	8. (1)	6. (3)	11. (3)	8. (4)	6. (4)
β_{23}	-8.4(9)	-9. (4)	-9. (2)	-9. (3)	-5. (3)

*Pressures are reported as kbar unless otherwise indicated.
**The x and z parameters are constrained to be 0 and 1/4, respectively. β_{12} and β_{23} are constrained to be 0.
†Parenthesized figures represent *esd's* of least units cited.
††All values of β are X 10^4.

Table 4: Interatomic distances and angles of the tetrahedral site in diopside at pressure

	1 atm	23.6*	35.2	45.5	53.0
Intra-tetrahedral distances (Å)					
Si-O(1C1)	1.602(3)**	1.598(3)	1.593(4)	1.591(4)	1.593(4)
Si-O(2C1)	1.589(1)	1.581(4)	1.586(3)	1.586(3)	1.587(3)
Si-O(3C1)	1.669(3)	1.670(3)	1.667(4)	1.666(3)	1.663(4)
Si-O(3C2)	1.687(3)	1.678(4)	1.680(4)	1.681(4)	1.676(4)
<Si-O>	1.637(1)	1.632(2)	1.632(2)	1.631(2)	1.630(2)
Inter-tetrahedral distances (Å)					
Si-Si	3.1089(3)	3.095(2)	3.0860(8)	3.0804(9)	3.075(1)
Intra-tetrahedral distances (Å)					
O(1C1)-O(2C1)	2.738 (5)	2.733 (5)	2.724 (7)	2.725 (6)	2.724 (6)
O(1C1)-O(3C1)	2.685 (4)	2.680 (4)	2.681 (6)	2.681 (5)	2.675 (6)
O(1C1)-O(3C2)	2.692 (9)	2.682 (8)	2.688 (12)	2.690 (10)	2.686 (10)
O(2C1)-O(3C1)	2.664 (1)	2.664 (4)	2.658 (2)	2.656 (3)	2.658 (3)
O(2C1)-O(3C2)	2.575 (1)	2.563 (5)	2.575 (2)	2.572 (3)	2.574 (3)
O(3C1)-O(3C2)	2.6445(3)	2.6288(9)	2.6257(5)	2.6201(6)	2.6166(7)
<O-O>	2.666	2.658	2.659	2.657	2.656
Intra-tetrahedral angles (deg)					
O(1C1)-Si-O(2C1)	118.21(9)	118.5(2)	117.9 (2)	118.1(2)	117.9(2)
O(1C1)-Si-O(3C1)	110.3 (2)	110.1(2)	110.6 (3)	110.7(3)	110.4(3)
O(1C1)-Si-O(3C2)	109.9 (3)	109.9(3)	110.3 (4)	110.5(3)	110.5(3)
O(2C1)-Si-O(3C1)	109.7 (1)	109.9(2)	109.5 (2)	109.4(2)	109.7(2)
O(2C1)-Si-O(3C2)	103.6 (2)	103.7(2)	104.0 (3)	103.8(2)	104.1(2)
O(3C1)-Si-O(3C2)	104.01(3)	103.5(1)	103.31(9)	103.0(1)	103.2(1)
Inter-tetrahedral angles (deg)					
Si-O(3)-Si	135.79(5)	135.1(1)	134.4(2)	133.9(2)	134.1(2)
O(3)-O(3)-O(3)	166.37(6)	165.7(3)	164.4(1)	164.0(2)	163.6(2)
Tetra. Vol. (Å^3)	2.230	2.208	2.210	2.206	2.203
Quad. Elong.	1.0067	1.0072	1.0066	1.0070	1.0066

*Pressures are reported as kbar unless otherwise indicated.
**Parenthesized figures represent *esd's* of least units cited.

(1969), although our lower R value results in higher precision of refined parameters. In addition, we have applied corrections for crystal X-ray absorption and secondary extinction to our data, which result in consistently higher equivalent isotropic temperature factors.

Comparisons of these data can be made with one other diamond-anvil study of a $C2/c$ pyroxene, a fassaite $[Ca_{0.97}Mg_{0.58}Fe^{2+}_{0.22}Al_{0.16}Ti_{0.06}(Si_{1.73}Al_{0.27})O_6]$, which is compositionally close to diopside (Hazen and Finger, 1977a, b) and with orthoenstatite (Ralph and Ghose, 1980). Fassaite is slightly more compressible than diopside. The zero-pressure bulk modulus (K_T) of diopside, calculated by fitting P-V data to the Birch–Murnaghan equation of state, is 1.13(3) Mbar, where the pressure derivative of K_T (K_T') equals 4.8(7) (Levien *et al.*, 1979). The values of K_T and K_T' for fassaite are 1.03(3) Mbar and 2.(1), respectively. Therefore the substitution of Al, Ti, and Fe, for Ca, Mg, and Si changes the compressibility of the structure. The orthoenstatite study did not have enough high-pressure data to determine K_T and K_T' values.

The three polyhedra that make up the diopside structure decrease in size irregularly as a function of pressure. The silicate tetrahedron in diopside contains four unique Si–O bonds, all of which decrease as a function of pressure, and two of which decrease more than one standard deviation (Table 4). The standard deviation of the average Si–O bond distance has been calculated by propagation of the errors on the four individual bond lengths. Using these errors, the average Si–O distance can be said to decrease significantly [1.637(1)Å → 1.630(2)Å]. Because average polyhedral bond distances show less scatter from data set to data set than individual bond lengths do, the standard deviation of the mean, although not strictly valid in a statistical sense, may be a reasonable deviation. A second reason we believe that real Si–O bond shortening has occurred is that the volume of the tetrahedron has decreased from

Table 5: Interatomic distances and angles of the M(1) octahedral site in diopside at pressure

	1 atm	23.6*	35.2	45.5	53.0
Intra-octahedral distances (Å)					
M(1)-O(1A1,B1)**	2.119(2)†	2.087(4)	2.091(3)	2.080(3)	2.075(3)
M(1)-O(1A2,B2)**	2.060(7)	2.050(6)	2.047(9)	2.043(7)	2.036(7)
M(1)-O(2C1,D1)**	2.051(2)	2.037(4)	2.023(3)	2.015(3)	2.011(3)
<M(1)-O>	2.076(2)	2.058(3)	2.053(3)	2.046(3)	2.041(3)
Inter-octahedral distances (Å)					
M(1)-M(1)	3.0952(5)	3.064(3)	3.056(1)	3.044(1)	3.036(2)
Intra-octahedral distances (Å)					
O(1A1)-O(1B1)	2.783 (5)	2.755(6)	2.748(8)	2.734(7)	2.727(8)
O(2C1)-O(2D1)	2.979 (4)	2.969(5)	2.965(7)	2.955(7)	2.958(7)
O(1A1)-O(2C1)**	3.019 (1)	2.975(5)	2.963(3)	2.950(3)	2.939(4)
O(1A1)-O(1A2)**	3.0527(7)	3.023(4)	3.027(2)	3.020(2)	3.015(2)
O(1A2)-O(2C1)**	2.881 (1)	2.863(4)	2.844(3)	2.837(3)	2.830(3)
O(1A2)-O(2D1)**	2.971 (8)	2.954(8)	2.936(11)	2.923(9)	2.913(9)
O(1A1)-O(1B2)**	2.808 (7)	2.780(8)	2.790(10)	2.781(8)	2.772(9)
<O-O>	2.935	2.910	2.903	2.893	2.885
Intra-octahedral angles (deg)					
O(1A1)-O(1B1)	82.1 (1)	82.6(2)	82.2(2)	82.2(2)	82.2(2)
O(1A1)-O(1A2)**	93.9 (1)	93.9(2)	94.0(2)	94.2(2)	94.3(2)
O(1A1)-O(2C1)**	92.6 (2)	92.6(2)	92.4(3)	92.2(2)	92.0(2)
O(1A1)-O(1B2)**	84.4 (1)	84.5(2)	84.8(2)	84.8(2)	84.8(2)
O(1A2)-O(2C1)**	89.0 (2)	88.9(2)	88.7(3)	88.7(2)	88.7(2)
O(1A2)-O(2D1)**	92.8 (1)	92.3(1)	92.2(1)	92.2(1)	92.0(1)
O(2C1)-O(2D1)**	93.17(8)	93.6(2)	94.3(2)	94.3(2)	94.7(2)
Octa. Vol. (Å^3)	11.848	11.538	11.460	11.334	11.238
Quad. Elong.	1.0054	1.0050	1.0053	1.0052	1.0053

*Pressures are reported as kbar unless otherwise indicated.
**This entry appears twice within the octahedron.
†Parenthesized figures represents *esd's* of least units cited.

Table 7: Unit-cell parameters of diopside at pressure

	a (Å)	*b* (Å)	*c* (Å)	β (deg)	*V* (Å^3)
1 atm	9.7456(7)	8.9198(8)	5.2516(5)	105.86(1)	439.13(6)
23.6(5)*	9.6809(7)	8.847 (1)	5.2169(3)	105.57(1)	430.41(7)
27. (1)	9.672 (2)	8.839 (2)	5.2115(6)	105.56(1)	429.2 (1)
35.2(5)	9.656 (1)	8.813 (1)	5.2026(3)	105.49(1)	426.69(8)
45.5(5)	9.630 (2)	8.785 (1)	5.1895(2)	105.37(1)	423.3 (1)
53.0(5)	9.612 (2)	8.765 (1)	5.1793(2)	105.32(1)	420.86(9)

*Parenthesized figures represent *esd's* of least units cited. Pressures are reported as kbar unless otherwise indicated.

2.230 to 2.203Å^3 (1.2 percent), a greater than 3σ change. Because calculations of quadratic elongation (Robinson *et al.*, 1971) (Table 4) show no change in the overall distortion of the tetrahedron, the volume decrease must be caused by bond shortening. The average tetrahedral bond distance in fassaite is longer at ambient conditions because of the 14 percent substitution of the larger Al^{3+} for the Si^{4+} cation, and compresses more than that in diopside (1.651 → 1.631Å); by 45 kbar the two minerals have the same average tetrahedral bond length. Also, the silicate tetrahedra in these two clinopyroxenes compress more than those in orthopyroxene.

The kinking of the silicate tetrahedral chain can be described either by the O(3)–O(3)–O(3) (bridging oxygen) angles or by the Si–O(3)–Si angles (Table 4). For diopside we observe a decrease in both these angles between 1 atm and 53 kbar, 135.79(5)° to 134.1(2)° in the former, and 166.37(6)° to 163.6(2)° in the latter. Therefore, a small amount of chain kinking occurs with increased pressure. Because the different cation polyhedra compress at different rates, and the silicate tetrahedra compress the least, the chains of tetrahedra must kink to retain structural integrity. The increased kinking of the chains of tetrahedra was not observed in fassaite (Hazen and Finger, 1977b); possibly the larger amount of compression shown by that tetrahedron made chain kinking unnecessary. In orthoenstatite, kinking of the B chains increases significantly with pressure whereas kinking only increases slightly in the A chains (Ralph and Ghose, 1980). In diopside the O(3) anion shows the greatest overall change from its original position in the structure. This movement accompanies the angular changes described above and, in addition, the O(3C1)–O(3C2) distance (using the nomenclature of Burnham *et al.*, 1967) within the silicate tetrahedron decreases twice as much as any other tetrahedral O–O distance.

Table 6: Interatomic distances of the M(2) polyhedral site in diopside at pressure

	1 atm	23.6*	35.2	45.5	53.0
M(2)-O(1A1,B1)**	2.363(2)†	2.357(4)	2.344(3)	2.337(3)	2.333(3)
M(2)-O(2C2,D2)**	2.346(8)	2.338(7)	2.336(10)	2.331(8)	2.327(8)
M(2)-O(3C1,D1)**	2.561(4)	2.546(5)	2.545(6)	2.538(5)	2.540(5)
M(2)-O(3C2,D2)**	2.721(4)	2.671(4)	2.639(6)	2.621(4)	2.609(5)
<M(2)-O>	2.498(3)	2.478(3)	2.466(3)	2.457(3)	2.452(3)
M(2) Vol. (Å^3)	25.749	25.160	24.859	24.585	24.462

*Pressures are reported as kbar unless otherwise indicated.
**This entry appears twice within the polyhedron.
†Parenthesized figures represent *esd's* of least units cited.

The M(1) octahedron, which contains Mg in diopside, also shows anisotropic compression with all three unique bonds (each appearing twice) compressing significantly (Table 5). The longest [M(1)–O(1A1)] and shortest [M(1)–O(2C1)] Mg–O bonds compress about the same amount (~2 percent), whereas the middle bond in length [M(1)–O(1A2)] compresses only a little more than half as much (~1.2 percent), and the average M(1)–O bond distance decreases 1.7 percent. The change in polyhedral volume of the octahedron of oxygens surrounding the Mg is 0.610Å^3 or 5.1 percent. The quadratic elongation of this octahedron remains 1.005, indicating that no polyhedral distortion takes place over the pressure range studied. Therefore, the change in volume must again be totally accounted for by the decreases in bond lengths. The changes in

the diopside M(1) polyhedron are quite different from that of fassaite. Hazen and Finger (1977b) report that the largest M(1) bonds compress the most, the middle length bonds next, and the shortest bonds do not change at all. The change in the average M(1)–O bond is only 1.1 percent, compared to 1.4 percent for diopside over a similar pressure range. The M(1) site is chemically the most different of the three cation sites between the fassaite and the diopside, with fassaite's M(1) containing 57% Mg, 21% Fe, 16% Al and 6% Ti (Hazen and Finger, 1977a). The chemical variation may account for this difference in structural behavior at pressure. The M(1) site of orthoenstatite, which also contains Mg, shows a similar amount of compression to M(1) in diopside (Ralph and Ghose, 1980).

The M(2) polyhedron of diopside has four unique bonds (each appearing twice), all of which compress significantly (Table 6). The longest bonds M(2)–O(3C2,D2) compress 4.1 percent, which is much more than any other in the structure; however, the second longest bonds [M(2)–O(3C1,D1)] are not the next most compressible. They compress the same percentage, 0.8, as the shortest M(2)–O bonds. Although the actual changes are slightly different, M(2) in fassaite shows essentially the same bond compression trends. The change in the average M(2)–O bond in diopside is 1.8 percent and the change in the volume of the M(2) polyhedron is 1.287Å^3 or 5.0 percent. For diopside, although the average bond distance for the M(2) polyhedron changes slightly more than that of M(1) (1.8% and 1.7%, respectively), the actual changes in polyhedral volumes are reversed with M(1) changing 5.1% and M(2) changing 5.0%. Therefore, larger cation polyhedra do not necessarily compress more than smaller ones, even within the same structure. In orthoenstatite the compression of the M(2) site is also essentially identical to that in diopside over 21 kbar, even though the chemical species in M(2) is Mg and not Ca (Ralph and Ghose, 1980).

There were apparent decreases in two of the equivalent isotropic temperature factors (Table 3), M(2) and O(2); the others remained unchanged over the 53 kbar pressure range studied. The ellipsoids of vibration for M(2) and O(2) conserve their orientations as pressure is increased and show most of their shortening along their longest principal axis.

Discussion

Comparison of the high-pressure structural changes between diopside and fassaite indicates differences that could be explained by the chemical contents of the respective polyhedra and/or by the presence of systematic errors in the experiments. For example, polyhedral compressibilities can be compared if they are calculated over the same pressure range or corrected back to zero-pressure values, as is done with P–V data to calculate bulk moduli. Hazen and Finger (1977b) report polyhedral compressibilities for fassaite of 0.27(T), 0.24[M(1)], and 0.39[M(2)] Mbar^{-1}. However, these values were calculated from the change of the average interatomic distance for each polyhedron, rather than for changes in polyhedral volumes. In Hazen and Finger (1979) a polyhedral bulk modulus (the inverse of compressibility) for M(2) (K = 0.85 Mbar, β = 1.18 Mbar^{-1}) was calculated from the change in average interatomic distance cubed, rather than changes in polyhedral volumes. We calculate polyhedral compressibilities from polyhedral volumes for both studies over the pressure range 0–45 kbar as follows:

Polyhedral Compressibilities (Mbar^{-1})

	Diopside	Fassaite
T	0.24	0.82
M(1)	0.95	0.69
M(2)	0.99	1.11

The differences between the compressibilities of the M(2) polyhedra probably are within the experimental error. It is at first surprising that the M(1) compressibility in diopside is similar to that for M(2), but examination of Tables 5 and 6 shows that six of the eight M(2)-O distances contract less than does the average M(1)-O distance, and only the largest two M(2)-O distances contract substantially more than the others. The only significant discrepancy between structures appears to be in the tetrahedral compressibilities. Although the Al content of the fassaite tetrahedron would account for some of the difference, it does not seem likely that the tetrahedral compressibility would be larger than that for M(1) in the same structure. Perhaps this is the result of a systematic error in Hazen and Finger's data.

Inverse effects of temperature and pressure

Although structural refinements of only a few structures are available at high temperatures and at high pressures (quartz, diopside, troilite, olivine, pyrope), the details of the structural changes are rarely exactly reciprocal. Part of the discussion of this behavior for diopside is in Levien *et al.* (1979), includ-

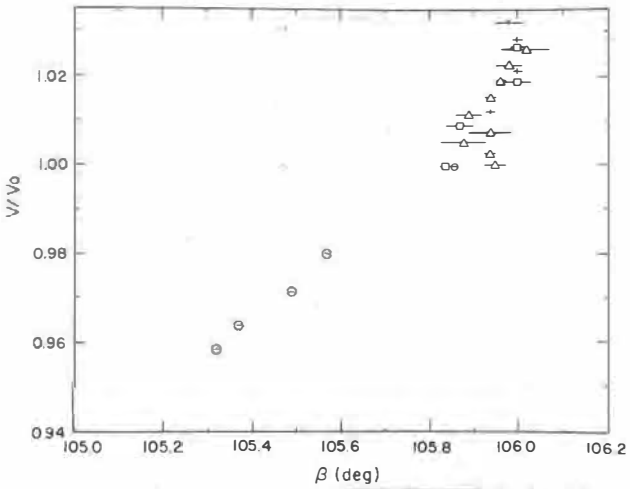

Fig. 1: Normalized unit-cell volume plotted against the β cell parameter. Circles represent our data; triangles are from Finger and Ohashi (1976); crosses are from Cameron *et al.* (1973); and squares are from Deganello (1973).

ing the calculation and comparison of unit-cell strain ellipsoids. Hazen and Prewitt (1977) predicted that minerals containing both Ca and Mg, such as diopside, will not show reciprocal behavior with increased temperature or pressure because the ratios of α/β (expansion/compression) for these two cations are so different, 0.058 kbar/deg for Mg and 0.071 kbar/deg for Ca. When these ratios are calculated for diopside using the Finger and Ohashi (1976) high-temperature results and our high-pressure values, these ratios are actually 0.044 kbar/deg for Mg and 0.058 kbar/deg for Ca. The magnitude of the difference between the values is similar, but the ratios themselves are not.

Figures 1-5 are plots of normalized unit-cell volume (V/V_0) as a function of changes shown by structural parameters. Rather than plotting temperature *vs.* pressure, because no scale exists which equates degrees and kbars, we have used changes in unit-cell volume as an analogous parameter. Where V is the unit-cell volume at T or P, and V_0 is the room-temperature–pressure value, V/V_0 will be greater than one for isobaric thermal expansion and less than one for isothermal compression. The data plotted are from three high-temperature studies, Deganello (1973)[3], Cameron *et al.* (1973), Finger and Ohashi (1976), and this high-pressure work. The Deganello study gave only unit-cell data, collected with high-temperature powder techniques; the other three studies provide structural data in addition to unit-cell data. Non-inverse behavior occurs in diopside's β unit-cell parameter, which is essentially invariant with temperature, but changes markedly with pressure. The parameter β decreases by 0.5° with 4.2 percent unit-cell volume compression, but changes less than 0.2° with a 3.2 percent expansion. To see if this non-inverse behavior is reflected in other structural parameters we have plotted normalized volume *vs.* the average Si–O distance (Fig. 2), the average M(1)–O distance (Fig. 3), the average M(2)–O distance (Fig. 4), and the two chain kinking angles, O(3)–O(3)–O(3) and Si–O(3)–Si (Fig. 5). The only parameter other than β to show a kink at ambient conditions is the average tetrahedral bond length; the other parameters show remarkably linear changes. Finger and Ohashi included three sets of bond distances, those uncorrected for thermal motion (plotted in Fig. 2), those corrected for parallel highly-correlated motion, and those corrected for noncorrelated motion. The first correction does not make a significant change in the average Si–O bond distance, but the second correction makes a large change, 0.025Å. If the distance for noncorrelated motion is correct, the silicate tetrahedron would still not exhibit reciprocal behavior because the change observed with temperature would then be larger instead of smaller than that seen with pressure.

No phase transition takes place or seems to be indicated by the structural data on diopside at high pressures. Because another pyroxene, pigeonite, although not compositionally close to diopside, shows a displacive phase transition with increased temper-

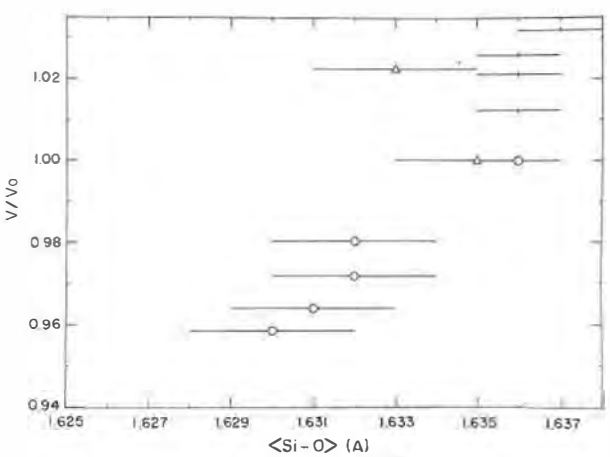

Fig. 2: Normalized unit-cell volume plotted against the average Si–O bond distance. Circles represent our data; triangles are from Finger and Ohashi (1976); crosses are from Cameron *et al.* (1973).

[3]The *b* room-pressure cell parameter in the Deganello study has been corrected to be 8.924Å. This change was reported as a personal communication by Finger and Ohashi (1976).

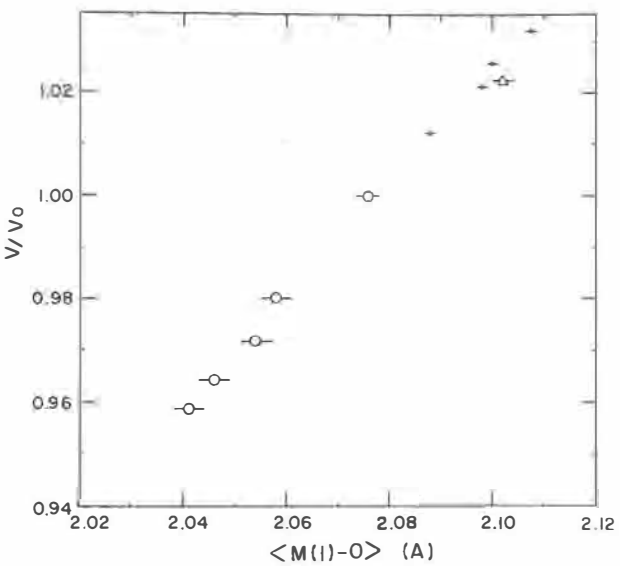

Fig. 3: Normalized unit-cell volume plotted against the average M(1)–O bond distance. Circles represent our data; triangles are from Finger and Ohashi (1976); crosses are from Cameron *et al.* (1973).

ature, ($P2_1/c \rightarrow C2/c$) (Brown *et* al., 1972), $C2/c$ pyroxenes might be expected to transform to the $P2_1/c$ structure with increased pressure. This transition seems unlikely because increased pressure favors higher coordination, and the $P2_1/c$ pyroxene has a six- and not eight-coordinated M(2) site. The fact that the longest M(2)–O bonds [M(2)–O(3C2,D2)] become shorter, making the M(2) site more tightly eight-coordinated, suggests that diopside will not transform to a primitive structure. However, high-pressure experiments on a $C2/c$ pyroxene along the Fs-Hd join of the pyroxene quadrilateral, close to the composition where Ohashi *et al.* (1975) show the transition to occur, would provide a better test of the inverse nature of this phase transition.

The difference in the changes shown by the equivalent isotropic temperature factors (B) with T or P requires discussion. For the high-temperature structural refinements the B's increase approximately 300–400 percent over the 3.2 percent change in unit-cell volume (1000°C). In sharp contrast, the B's change very little with increased pressure, the maximum change being 17 percent during 4.2 percent volume compression. Therefore comparable changes in unit-cell volumes, and thus polyhedral volumes are not the major contributing factor to the B's. Increased temperature simultaneously increases the volume and the energy of the structure, and thus excites more lattice vibrations. An additional related effect of increased T is to increase the anharmonic motion of these vibrations; this motion is responsible for thermal expansion. Therefore, it is not structural volume as much as energy that controls the magnitudes of the temperature factors.

Elasticity

The primary discussion of the elasticity of diopside has been included in Levien *et al.* (1979). Values for the bulk modulus, K_T, and its pressure derivative, K'_T, calculated by fitting the P–V data (Table 7) to a Birch–Murnaghan equation of state, were reported as K_T = 1.13(3) Mbar and K'_T = 4.8(7). Using techniques of Bass *et al.* (1979), we have calculated a weighted fit for the data [K_T = 1.14(4) Mbar and K'_T = 4.5(1.8)]. These values and corresponding standard deviations better reflect the true accuracy of the data, as the P–V data seem to fall fortuitously close to the analytical curve calculated by the unweighted fit.

If the diopside structure is modeled as linked polyhedra with "void" space between them, the sums of the volumes of these polyhedra comprise 38 percent of the unit-cell volume at all pressures studied. There are no large changes in the "voids" that can be specifically correlated to the structural compression, and the voids compress at about the same rate as the polyhedra. Levien *et al.* (1979) hypothesized that the single-crystal elastic moduli of diopside are consistent only with a model of compression controlled by

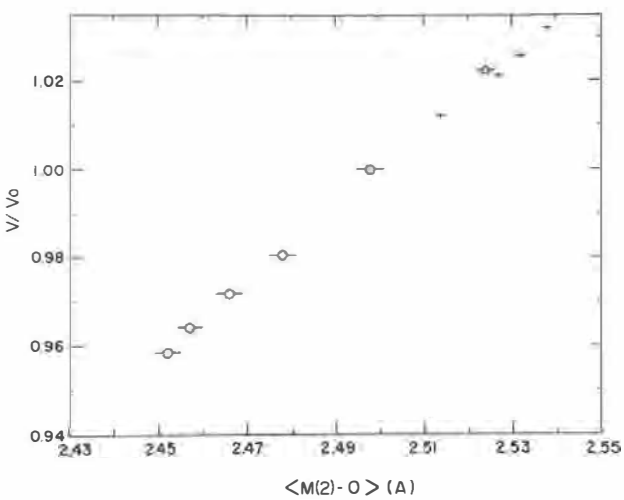

Fig. 4: Normalized unit-cell volume plotted against the average M(2)–O bond distance. Circles represent our data; triangles are from Finger and Ohashi (1976); crosses are from Cameron *et al.* (1973).

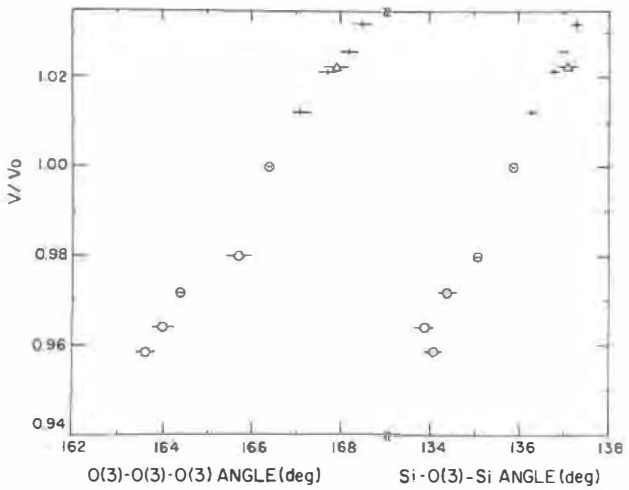

Fig. 5: Normalized unit-cell volume plotted against the two chain kinking angles, O(3)–O(3)–O(3) and Si–O(3)-Si. Circles represent our data; triangles are from Finger and Ohashi (1976); crosses are from Cameron *et al.* (1973).

the deformable six- and eight-fold coordinated cation polyhedra. This study confirms that hypothesis, as changes in Si–O bond lengths and silicate-chain kinking angles are fairly small. If the decrease in volume is not caused by structural channels closing or silicate-chain movements, the M–O distances must control the compression.

As reported in Levien *et al.* (1979), the unit-cell directions in diopside that correspond to the three principal axes of a strain ellipsoid describing the compression are very close to those that describe the thermal expansion reported by Finger and Ohashi (1976). However, the magnitudes of the changes are different, with $\epsilon_3 \cong \epsilon_2 \cong 2\epsilon_1$ for the compression data and $\epsilon_1 \cong 2\epsilon_2 \cong 4\epsilon_3$ for the expansion data, where ϵ's are the linear strain coefficients in the three principal directions. Because b is an axis of symmetry, one of these directions is constrained to be parallel to it; the other two axes must lie in the a–c plane. With both high T and P, the direction showing the greatest change is $\parallel$ to b (for the high-pressure data $\epsilon_3 \cong \epsilon_2$ and therefore b is sometimes $\parallel$ to ϵ_2); the direction showing the least change is in the a–c plane, rotated 37° from c toward a. Finger and Ohashi point out that the direction of minimum expansion is nearly parallel to the two bonds [M(2)–O(2C2, D2)] which do not expand significantly with increased temperature. One cause for the difference in the magnitudes of the ϵ's shown above is that these bonds do compress significantly with pressure. In addition to these two bonds, there are two M(1)–O bonds that run nearly parallel to this direction [M(1)–O(1A2,B2)]. These bonds are also very stiff, showing the same percentage compression as the M(2)–O(2C2,D2) bonds. Therefore ϵ_1 not only has a large number of M–O bonds parallel to it, but these bonds are fairly rigid. The parameters ϵ_2 and ϵ_3 exhibit approximately the same amount of change, with the compressible M(2)–O(3) bonds contributing to the decrease of both. These bonds run almost at right angles to ϵ_1 and approximately 45° between ϵ_2 and ϵ_3. In addition, ϵ_2 and ϵ_3 nearly bisect any O–M–O angles through which they pass, and have no M–O bonds parallel to them.

Conclusions

1. The three polyhedra that comprise the diopside structure change anisotropically, with the silicate tetrahedron showing a very small but significant compression, and both the M(1) and M(2) polyhedra showing approximately five percent volume compression. The fact that M(1) and M(2) change approximately the same amount suggests that larger polyhedra do not necessarily compress more than small ones, even within the same structure.

2. Although diopside and fassaite are very similar structurally and chemically, there are substantial differences in their compressions. The diopside shows less tetrahedral compression, more octahedral compression, and more silicate chain kinking.

3. Equivalent isotropic temperature factors change very little with increased pressure; only the B's of the M(2) and O(2) ions show significant decreases.

4. High-temperature and high-pressure structural studies suggest that some structural features show inverse behavior with volume changes caused by T and P, whereas others do not. Figures 1 and 2 show noninverse behavior of the β cell parameter and the average Si–O bond distance; Figures 3, 4, and 5 show reciprocal behavior for the average M(1)–O bond, the average M(2)–O bond, and the chain-kinking angles. No phase transition similar to that of high to low pigeonite is indicated by the high-pressure data.

Unit-cell volume changes have only a secondary effect on equivalent isotropic temperature factors. Increased T has a much larger effect on the magnitude of the B's than does increased pressure that causes a similar percentage change in unit-cell dimensions.

5. Using a weighted fit of the P–V data to the Birch–Murnaghan equation of state, we have recalculated the bulk modulus and its pressure derivative (and corresponding standard deviations) to be 1.14(4) Mbar and 4.5 (1.8), respectively. These higher

standard deviations better reflect our true confidence in the values of these moduli.

6. The compression of the structure is controlled by the directions and compressibilities of the bonds in the M(1) and M(2) polyhedra, and not by the chains of silicate tetrahedra. The least compressible M–O bonds can be correlated with the direction of minimum compression in the diopside structure; the most compressible bonds [M(2)–O(3C2,D2)] are oriented 45° between the two principal axes showing the greatest compression. Although we may not yet be able to predict structural changes with temperature and pressure, there do seem to be clear patterns of changes emerging from the few structures that have been studied.

Acknowledgments

We thank J. D. Bass for developing the program to calculate the elastic parameters, and J. D. Bass, R. C. Liebermann, D. J. Weidner, H. E. King, and L. W. Finger for helpful discussions about this work. We also acknowledge A. E. Bence for the microprobe analysis of the sample, and L. W. Finger for his help in collecting the unit-cell data at 27 kbar. This research was supported by the NSF grant EAR77-13042. The first author also gratefully acknowledges a predoctoral fellowship awarded to her by the American Association of University Women Educational Foundation.

References

Bass, J. D., Liebermann, R. C., Weidner, D. J. and Finch, S. J. (1979) Elasticity data from acoustic and volume compression experiments. (abstr.) EOS, 60, 386.

Brown, G. E., Prewitt, C. T., Papike, J. J. and Sueno, S. (1972) A comparison of the structures of low and high pigeonite. Journal of Geophysical Research, 77, 5778–5789.

Burnham, C. W., Clark, J. R., Papike, J. J. and Prewitt, C. T. (1967) A proposed crystallographic nomenclature for clinopyroxene structures. Zeitschrift für Kristallographie, 125, 109–119.

Cameron, M., Sueno, S., Prewitt, C. T. and Papike, J. J. (1973) High temperature crystal chemistry of acmite, diopside, hedenbergite, jadeite, spodumene, and ureyite. American Mineralogist, 58, 594–618.

Clark, J. R., Appleman, D. E. and Papike, J. J. (1969) Crystal-chemical characterization of clino-pyroxenes based on eight new structure refinements. Mineralogical Society of America Special Paper Number 2, 31–50.

Deganello, S. (1973) The thermal expansion of diopside. Zeitschrift für Kristallographie, 137, 127–131.

Finger, L. W. and Ohashi, Y. (1976) The thermal expansion of diopside to 800°C and a refinement of the crystal structure at 700°C. American Mineralogist, 61, 303–310.

Hamilton, W. C. (1974) Tests for statistical significance. In J. A. Ibers and W. C. Hamilton, Eds., International Tables for X-Ray Crystallography, Vol. IV, p. 285–310. Kynoch Press, Birmingham, England.

Hazen, R. M. and Finger, L. W. (1977a) Crystal structure and compositional variation of Angra dos Reis fassaite. Earth and Planetary Science Letters, 35, 357–362.

Hazen, R. M. and Finger, L. W. (1977b) Compressibility and structure of Angra dos Reis fassaite to 52 kbar. Carnegie Institution of Washington Year Book, 76, 512–515.

Hazen, R. M. and Finger, L. W. (1977c) Modifications in high-pressure single-crystal diamond-cell techniques. Carnegie Institution of Washington Year Book, 76, 655–656.

Hazen, R. M. and Finger, L. W. (1979) Bulk modulus-volume relationship for cation-anion polyhedra. Journal of Geophysical Research, 84, 6723–6728.

Hazen, R. M. and Prewitt, C. T. (1977) Effects of temperature and pressure on interatomic distance in oxygen-based minerals. American Mineralogist, 62, 309–315.

Levien, L., Weidner, D. J. and Prewitt, C. T. (1979) Elasticity of diopside. Physics and Chemistry of Minerals, 4, 105–113.

Levien, L., Prewitt, C. T. and Weidner, D. J. (1980) Structure and elastic properties of quartz at pressure. American Mineralogist, 65, 920–930.

Merrill, L. and Bassett, W. A. (1974) Miniature diamond anvil pressure cell for single crystal X-ray diffraction studies. Review of Scientific Instruments, 45, 290–294.

Ohashi, Y., Burnham, C. W. and Finger, L. W. (1975) The effect of Ca–Fe substitution on the clinopyroxene crystal structure. American Mineralogist, 60, 423–434.

Ralph, R. L. and Ghose, S. (1980) Enstatite, $Mg_2Si_2O_6$: Compressibility and crystal structure at 21 kbar. (abstr.) EOS, 61, 409.

Robinson, K., Gibbs, G. V. and Ribbe, P. H. (1971) Quadratic elongation: a quantitative measure of distortion in coordination polyhedra. Science, 172, 567–570.

Manuscript received, October 17, 1979;
accepted for publication, October 6, 1980.